

Raman spectroscopy and structural properties of $\text{In}_x\text{Bi}_{40-x}\text{Se}_{60}$ system

S.A. Saleh^{a,b,*}, E.M.M. Ibrahim^a, M.M. Wakkad^a

^a Physics Department, Faculty of Science, Sohag University, Sohag 82524, Egypt

^b Physics Department, College of Science & Arts, Najran University, P.O. 1988 Najran, Saudi Arabia

ARTICLE INFO

Article history:

Received 8 March 2012

Received in revised form 28 March 2013

Accepted 28 March 2013

Available online 8 April 2013

Keywords:

X-ray diffraction

Raman spectroscopy

Energy dispersive spectroscopy

ABSTRACT

$\text{In}_x\text{Bi}_{40-x}\text{Se}_{60}$ ($x = 1.6, 4.4, 7, 10$ and 13.2) alloys were synthesized by melt-quenching technique. The X-ray diffraction and Raman spectroscopy investigations confirm that the materials are in single phase. Archimedes method and Energy Dispersive Spectroscopy (EDS) have been used for density and chemical characterization of the obtained materials. Indium content dependences of different parameters such as the density (D), the compactness (δ), and the average coordination number (Z) have been investigated and discussed in light of chemical order network and topological models.

© 2013 Elsevier B.V. All rights reserved.

1. Introduction

Recently, there is a substantial interest in the preparation and characterization of chalcogenide materials due to their wide applications in modern electronics, optoelectronics, integrated optics, electrophotography, solar cells, electrical and optical memory devices and modern thermoelectric cooling modules [1–4]. This variety of applications stem from their fascinating physical properties which are closely related to their structure and composition. Bi_2Se_3 is a member of the group of compounds which are highly feasible for thermoelectric power applications [5]. For using as thermoelectric generator, the Bi_2Se_3 alloy should be in single crystal or polycrystalline phase and its physical properties should be well defined. Actually, various factors can tune the physical properties of the materials. Among all, doping with suitable foreign atoms is considered a main issue in this approach. This may explain why studying the effect of various dopants on the physical properties of Bi_2Se_3 is interesting in both basic and applied research fields. Adding a third element to the binary alloy creates compositional and configurational disorder in the material and thus facilitates understanding of the structural properties. Therefore, the structural studies of $\text{In}_x\text{Bi}_{40-x}\text{Se}_{60}$ alloy with systematic variation of indium content can be advantageous for gaining important insight in the associated change of the structure property.

Several experimental techniques such as X-ray diffraction (XRD), scanning electron microscopy (SEM), Raman spectroscopy,

electrical resistivity and scanning calorimetry were used to study the structure of chalcogenide alloys [6–10]. Structural properties of these solids could be explained with topological models [11], chain crossing model (CCM) [12], random covalent network model (RCNM) [13], chemical ordered network model (CONM) [14] and molecular models [15]. In these models, some of the properties were discussed in terms of the average coordination number, which is indiscriminate in species of the valence bond.

In this work we have reported and discussed the results of the XRD and Raman spectroscopy investigations of a series of $\text{In}_x\text{Bi}_{40-x}\text{Se}_{60}$ with $1.6 \leq x \leq 13.2$ aiming to study the effect of In content on the structure. We also have reported a wide range of properties of these alloys including material density, average atomic volume, average coordination number, number of constraints and heat of atomization. The possible consequences of the atomic structure in controlling these physical properties have been discussed.

2. Experimental details

A series of $\text{In}_x\text{Bi}_{40-x}\text{Se}_{60}$ ($x = 1.6, 4.4, 7, 10$ and 13.2) were prepared from high purity elements using the melt-quenching technique. Appropriate atomic weight percentages of the three elements were mixed and charged in 8 mm diameter silica tubes sealed under vacuum of 10^{-5} torr. The sealed quartz ampoules were kept in a furnace at fixed temperature 1073 K for 48 h with frequent agitation to realize homogeneous mixing of the precursors. The tubes with the molten were quenched in an ice–water mixture. Then the quartz tubes were broken and the ingots of the samples were extracted and grinded thoroughly for 2 h. The powders were sieved using a sieve with a mesh size of 63 μm . Micro-structure

* Corresponding author at: Physics Department, Faculty of Science, Sohag University, Sohag 82524, Egypt. Tel.: +20 9324601159; fax: +20 9324601159.

E-mail address: saleh2010@yahoo.com (S.A. Saleh).

Table 1

Literature data of the constituent elements in the synthesized alloys.

Property	Bi	Se	In
Density (g/cm ³)	9.747	4.79	7.31
Coordination number	3	2	4
Atomic radius (Å)	1.545	1.16	1.626
Atomic mass (gm atom)	208.98	78.96	114.82
Bond energy (kcal/mol)	47.9	44.04	21.02
Electronegativity	1.9	2.55	1.78

observation and chemical analysis were performed by using a field emission scanning electron microscope (FESEM) (JEOL JSM-7600F) combined with an energy dispersive spectroscopy (EDS). The XRD analysis was carried out using a PANalytical X'PertPRO diffractometer at room temperature with Cu (K_{α}) radiation ($\lambda = 1.54059 \text{ \AA}$). The Raman spectra were obtained using (Perkin Elmer) Raman spectrometer in the wavenumber region $500\text{--}60 \text{ cm}^{-1}$ at room temperature. The density of the sample (D) was measured using Archimedes balance method. The pellets used for density measurement were carefully chosen to be free from cracks and cleaned by ethanol to remove any surface contamination. Note that, for each composition the measurement was repeated four times and the obtained D values were averaged. The density values were used for calculating some physical parameters and some required physicochemical properties (see Table 1) reported in literature [16–22] for Bi, Se and In elements were exploited. The compactness (δ) was calculated according to the formula [23,24]: $\delta = \frac{\sum_i C_i A_i / D_i - \sum_i C_i A_i / D}{\sum_i C_i A_i / D}$,

where C_i , A_i , and D_i are the atomic fraction, atomic weight and atomic density of the i th element of the pellet and D is the measured density of the sample. The accuracy of the density measurement, and consequently the compactness (δ) was estimated to be better than ± 0.01 .

3. Results and discussion

Table 2 presents the atomic percentage of the In, Bi, and Se elements for the prepared compositions measured by the EDS technique. Noteworthy, the estimated average deviation from the desired stoichiometry of each composition does not exceed 2% in atomic fraction. The average coordination number Z of a ternary $\text{In}_{\alpha}\text{Bi}_{\beta}\text{Se}_{\gamma}$ system is defined by the expression [25]: $Z = \frac{4\alpha+3\beta+2\gamma}{\alpha+\beta+\gamma}$

where α , β , and γ are the atomic percentages of In, Bi, and Se, while 4, 3, and 2 are their coordination numbers. The coordination number Z characterizes the electronic properties of the semiconducting materials, and indicates the bonding character in the nearest-neighbor region [26]. The Z values (presented in Table 2) were used to estimate the number of constraints N_s , which represents a sum of the radial and angular valence force constraints [27]. For a material with a given coordination number Z , two components can contribute to the constraints $N_s(Z)$ which are the bond-stretching $N^{\alpha}(=Z/2)$ and the bond-bending $N^{\beta}(=2Z-Z3)$ [28]. Accordingly, the $N_s(Z)$ is given as, $N_s = (5/2)Z - 3$

The stoichiometry deviation can be represented by a parameter R which is expressed as the ratio of the covalent bonding possibilities of chalcogen atoms to that of non-halogen atoms. For a ternary

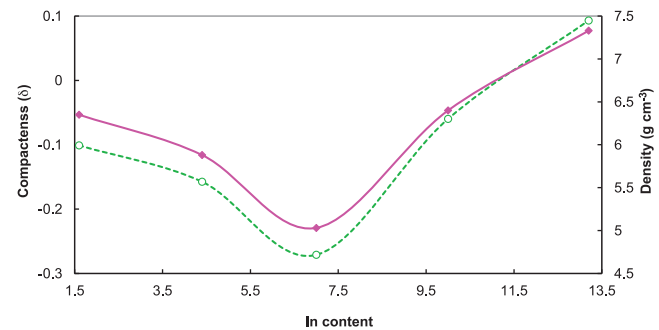


Fig. 1. Compactness (δ) and density (D) of $\text{Bi}_{40-x}\text{In}_x\text{Se}_{60}$ materials vs. In content.

$\text{In}_{\alpha}\text{Bi}_{\beta}\text{Se}_{\gamma}$ system, the parameter R is given by the following relation [29]:

$$R = \frac{2\gamma}{4\alpha + 3\beta}$$

For R larger than unity, the system is chalcogen-rich (there are hetero-polar bonds and chalcogen–chalcogen bonds present) while for R smaller than unity, the system is chalcogen-poor (there are only hetero-polar bonds and metal–metal bonds present).

Z , N_s , δ , and R of the nominal bulk $\text{In}_x\text{Bi}_{40-x}\text{Se}_{60}$ ($1.6 \leq x \leq 13.2$) compositions are tabulated in Table 2. Fig. 1 illustrates the In content dependence of D and δ for the compositions at hand. The data reveal that D and δ have clear inflection points at $x=7$. This can be largely explained within the frame work of chemically ordered network model (CONM) proposed by Bicerano and Ovshinsky [14]. According to this model, the composition structure is assumed to be composed of cross-linked structural units of stable chemical compounds (hetero-polar bonds) of the system and excess of the elements (homo-polar bonds). Due to the chemical ordering, features like extremum and/or change in slope or kink [30] occur for the various properties at the tie line composition or the chemical threshold of the system. For this composition, the system structure is made up of cross-linked pyramidal-like BiSe_3 structural unit which consist of energetically favored heteropolar bonds only. Heteropolar bonds thus have pre-eminence over homopolar bonds and bonds are formed in the sequences of decreasing bond energy until all the available valences of the atoms are saturated. Each constituent is coordinated by $8-N$ atoms, where N is the number of electrons in outer shell and this is equivalent to neglecting the dangling bonds and the other valence defects. As shown in Table 2, a minimum in the compositional dependence of D and δ is attained at $Z=2.47$ which can be attributed to a change from an elastically floppy type to a rigid type. According to the constrain theory [31], the investigated compositions are over-coordinated, stressed-rigid and with lower connectivity, as the values of Z are larger than 2.4. These observations indicate that the effects of chemical ordering are also presented in this system along with the overall topological effects. In other words, the dependence of D and δ on In content and Z has been examined in light of topological and chemical ordered network models. It is evident that both D and δ values are affected by the interaction between the constituent elements and the connectivity of a glassy network. The stability of the network depends

Table 2

Physical properties of $\text{Bi}_{40-x}\text{In}_x\text{Se}_{60}$ compositions.

Composition	$D \text{ g cm}^{-3}$	δ	Z	N_s	Parameter R	$G_s \text{ (nm)}$	$\varepsilon (10^{-4})$	$\rho (10^{10} \text{ cm}^{-2})$
$\text{Bi}_{38.4}\text{In}_{1.6}\text{Se}_{60}$	6.35	-0.10099	2.42	3.05	0.99	62.7	5.53	2.54
$\text{Bi}_{35.6}\text{In}_{4.4}\text{Se}_{60}$	5.88	-0.15750	2.44	3.10	0.96	86.8	3.99	1.33
$\text{Bi}_{33}\text{In}_7\text{Se}_{60}$	5.03	-0.27103	2.47	3.18	0.94	104.7	3.31	0.91
$\text{Bi}_{30}\text{In}_{10}\text{Se}_{60}$	6.4	-0.05981	2.50	3.25	0.92	63.1	5.49	2.51
$\text{Bi}_{26.8}\text{In}_{13.2}\text{Se}_{60}$	7.33	0.09304	2.53	3.33	0.90	59.8	5.8	2.8

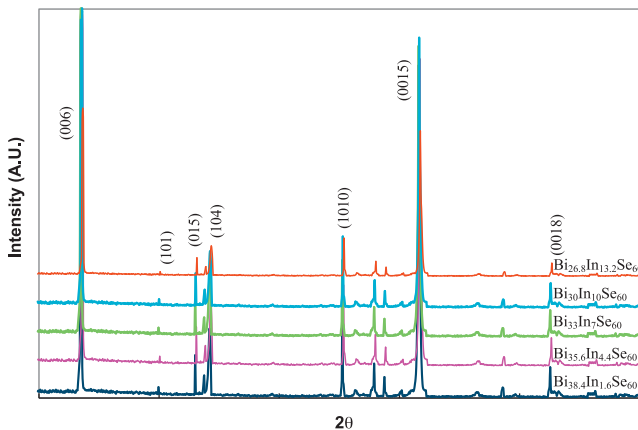


Fig. 2. XRD patterns of (S1) $\text{Bi}_{38.4}\text{In}_{0.4}\text{Se}_{60}$, (S2) $\text{Bi}_{35.6}\text{In}_{4.4}\text{Se}_{60}$, (S3) $\text{Bi}_{33}\text{In}_7\text{Se}_{60}$, (S4) $\text{Bi}_{30}\text{In}_{10}\text{Se}_{60}$ and (S5) $\text{Bi}_{26.8}\text{In}_{13.2}\text{Se}_{60}$ compositions.

on the atomic arrangements; the stronger the chemical bonds and the shorter the bond length, the smaller the average atomic volume and the larger the compactness of the network.

The X-ray diffraction (XRD) patterns of $\text{In}_x\text{Bi}_{40-x}\text{Se}_{60}$ ($x = 1.6, 4.4, 7, 10$ and 13.2) system are depicted in Fig. 2. The reflection peaks correspond to the rhombohedral tetradymite structure (see JCPDS card no. 33-0214) with space group symmetry R3 m and consists of five stacked layers of atoms along the c-axis of the hexagonal [32,33]. Note that, no indication of other structures or impurities was detected. The sharpness and high intensity of the prominent peaks suggest that the prepared samples are well crystalline. The minor shift observed in the peaks positions may indicate to small changes in the lattice parameters because the difference in ionic radius of Bi^{3+} and In^{3+} ions which causes a slight increase in the rhombohedral unit cell volume [34]. The diffraction peaks related to $(00l)$ planes (including (006) , (0015) , and (0018)) are much more intense than others indicating that the c-axis of the grains were preferentially oriented parallel to the pressing direction. The orientation degree of the $(00l)$ planes can be determined by the orientation factor F , which can be calculated using Lotgering method [35]. $F = (P - P_0)/(1 - P_0)$, $P_0 = I_{(00l)} / \sum I_{(hkl)}$, $P = I_{(00l)} / \sum I_{(hkl)}$, where P and P_0 are the ratios of the integrated intensities of all $(00l)$ planes to those of all (hkl) planes for the preferentially and non-preferentially orientated directions, respectively. The orientation factor (F) varies from 0 for an entirely non-oriented sample to 1 for a completely orientated one. According to Lotgering method, it was found that F changes slightly between 0.75 and 0.79 indicating an insignificant influence of In content on the orientation factor. The microstructural parameters like grain size (G_s), lattice strain (ε) and dislocation density (ρ) have been calculated and presented in Table 2. The grain size (G_s) of the crystallites in the specimen of various doping content was estimated from (006) plane using Sherrer's equation [36]: $G_s = 0.89\lambda/\beta \cos\theta$ where, β is the full width at half maximum (FWHM) of the diffraction peak corresponding to the Bragg angle θ and λ (wavelength of the Cu K_α radiation) = 1.54059\AA . The lattice strain (ε) is determined using the relation [37], $\varepsilon = \beta \cos\theta/4$ and the value of dislocation density (ρ) was deduced from the expression [38] $\rho = 1/G_s^2$. The data reveal that the crystallite size of Bi_2Se_3 nanoparticles first increases with In increase till $x = 7\%$ and then decreases while the lattice strain changes oppositely. Generally, the broadening of the diffraction peaks depends upon the particle size and lattice strain. The very fine particle size in nanoscale is expected to result in lattice strain [39]. The strain in nanocrystallines is attributed to the grain interior dislocations and grain boundary dislocations [40]. However, it can also be due to excess volume of grain boundaries resulted

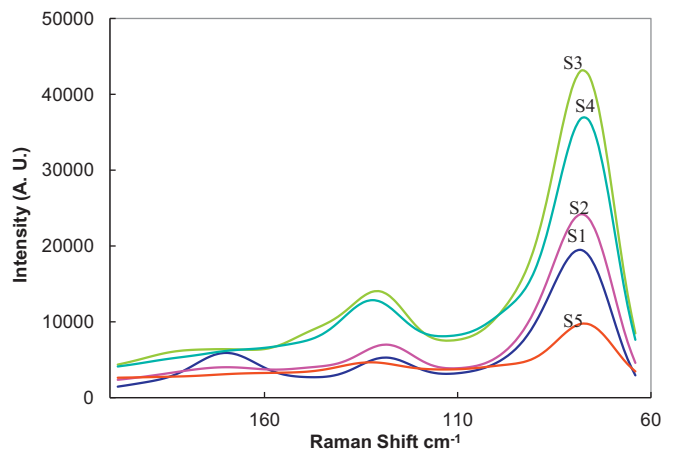


Fig. 3. Raman spectra of (S1) $\text{Bi}_{38.4}\text{In}_{0.4}\text{Se}_{60}$, (S2) $\text{Bi}_{35.6}\text{In}_{4.4}\text{Se}_{60}$, (S3) $\text{Bi}_{33}\text{In}_7\text{Se}_{60}$, (S4) $\text{Bi}_{30}\text{In}_{10}\text{Se}_{60}$ and (S5) $\text{Bi}_{26.8}\text{In}_{13.2}\text{Se}_{60}$ compositions.

from vacancies and vacancy clusters. Further, it arises from displacement of unit cell about its normal position and is often caused by dislocations, surface restructuring, lattice vacancies, interstitials, substitutions, etc., which are very common in nanocrystals [41].

Raman spectra study provides valuable information about the structure of materials because of the extreme sensitivity of the vibrational spectroscopy to the electronic structural changes. Thus, it is instructive to consider the vibrational bands in $\text{Bi}(\text{In})\text{Se}_3$ trigonal pyramidal groups for interpreting the $\text{Bi}(\text{In})-\text{Se}$ modes on the basis of molecular model [15]. Ideally, the four-atom groups constituting an $\text{Bi}(\text{In})\text{Se}_3$ pyramid would have four normal modes of vibration: a symmetric stretching vibration $\nu_1(A_1)$, a symmetric bending vibration $\nu_2(A_1)$, an anti-symmetric stretching vibration $\nu_3(E)$ and an anti-symmetric bending vibration $\nu_4(E)$. The bond energies of various possible heteropolar $\text{Bi}-\text{Se}$, $\text{In}-\text{Se}$, and $\text{Bi}-\text{In}$ bonds have been calculated on the basis of the relation proposed by Pauling [42]:

$$E_{A-B} = (E_{A-A}E_{B-B})^{0.5} + 30(X_A - X_B)^2$$

where E_{A-A} and E_{B-B} are the single-bond energies and X_A and X_B are the electronegativities of atoms A and B, respectively. As shown in Table 2, values of R were found to be smaller than unity of the prepared system suggesting Se-poor materials. There are only hetero-polar bonds and metal-metal ($\text{Bi}-\text{Bi}$) bonds present. From an energy point of view, heteropolar bonds are more favorable than homopolar bonds. The spectra of these alloys could be described as a result of superposition of the spectra of their structural components. The Raman spectra for $\text{Bi}-\text{In}-\text{Se}$ system has been discussed by taking the formation of two basic structural units, $\text{Bi}(\text{In})\text{Se}_3$ pyramids with threefold coordinated Bi (In) atom at the apex. The vibrational bands reported in the literature for their crystalline accompaniment were taken as references for the discussion of the spectrum [15,43,44]. The Raman spectra of our system are depicted in Fig. 3. For the sample of $x = 1.6$ (S1), the main bands appear at ~ 78 , ~ 130 and $\sim 170\text{ cm}^{-1}$. The first two bands may represent mixed contributions from $\text{Bi}-\text{Se}$ and $\text{In}-\text{Se}$ modes while the last band was assigned to $\text{Bi}-\text{Bi}$ modes as in the Se-deficient compounds. The lowest frequency band near 78 cm^{-1} is assigned to the $\nu_4(E)$ mode of the $\text{Bi}(\text{In})\text{Se}_3$ trigonal pyramidal groups while the band at 130 cm^{-1} is ascribed to $\nu_2(A_1)$ resulted from a symmetric bending of $\text{Bi}(\text{In})\text{Se}_3$ pyramids [15]. The band near 170 cm^{-1} band has two possible origins since it can be attributed either to the stretching mode of the $\text{Se}_3\text{In}-\text{InSe}_3$ or to the A_{1g} mode in $c\text{-Bi}_2\text{Se}_3$ [43]. This band has been ascribed to the homopolar $\text{Bi}-\text{Bi}$ in $\text{Se}_3\text{Bi}-\text{BiSe}_3$ structural units [44] resulted from the Se deficiency. This result is in excellent

agreement with the less than unity value of R and CONM. When the In content increases, there is a progressive decrease of the amplitude of the band located at 170 cm^{-1} indicating a decrease of the number of homopolar Bi–Bi bonds and increase in the number of heteropolar In–Se bonds. Moreover, in addition to the main bands which appear at 76 and 128 cm^{-1} , a very low intensity peak around 168 cm^{-1} is also observed for the S3 ($x=7$) sample. The Raman spectra of $\text{Bi}_{30}\text{In}_{10}\text{Se}_{60}$ (S4) and $\text{Bi}_{26.8}\text{In}_{13.2}\text{Se}_{60}$ (S5) are characterized by two bands at 76 and 128 cm^{-1} . These results match with the density of the samples (see Table 2).

Some systematic changes in the vibrational band frequencies and intensities with the composition variation are observed and shed light on the structural evolution of our compositions. To be specific, the decrease of the 170 cm^{-1} band and the increase of the two Raman active modes at ~ 80 and $\sim 130\text{ cm}^{-1}$ bands are closely related to the increase of the indium concentration in the specimens. In agreement with the evolution of the density in the investigated system, it is confirmed that D is influenced more by an increase of In–Se bonds than by an increase of Bi–Se bonds. The vibration spectra must correspond primarily to vibrational modes involving Bi(In)–Se bonds because Se–Se bonds would be highly unexpected in these Se-poor materials and stretching modes of Bi–Bi homopolar bonds are located at significantly higher frequencies. In the other words, the basic structural unit of ternary (Bi–In–Se) system is expected to be $\text{Bi}(\text{In})\text{Se}_3$ pyramids with threefold coordinated Bi(In) atom at the apex which are weakly coupled through two atomic Se–Se bridging groups [44]. Also, it was found that the changes occur systematically with increasing the In content.

Moreover, Raman spectroscopy was performed to investigate the effect of indium substitution on the lattice vibration and chemical bonding nature in layered $(\text{Bi}, \text{In})_2\text{Se}_3$ compounds. The $(\text{Bi}, \text{In})_2\text{Se}_3$ crystal structure has a hexagonal conventional unit cell with a $-\text{(Se}^1\text{—Bi/In—Se}^2\text{—Bi/In—Se}^1)-$ layer stacked along the c_{H} axis, with $\text{Se}^1\text{—Se}^1$ bond of van der Waals type [45]. Here, superscripts (1) and (2) denote two different chemical states for the anions. The outmost atoms Se^1 are strongly bonded to three planar Se^1 and three Bi/In metal atoms of the same quintuple layers and weakly bonded to three Se^1 atoms of the next fivefold. The binding between adjacent Se^1 layers originates mostly from the weak van der Waals forces although other long-range Coulomb forces play a role in the bonding. The stronger bonds inside the quintuple layers are of the covalent or partially ionic nature. The presence of the van der Waals gap between the quintuples results in preferential cleavage plane between the adjacent Se^1 layers. According to the group theory analysis [46], the investigated system possesses four Raman active modes of $2E_g + 2A_{1g}$. Both E_g and A_{1g} modes are twofold degenerate: in E_g , the atoms vibrate in the basal plane, while in A_{1g} , the atoms vibrate along c_{H} [47]. The A_{1g}^1 and E_g^1 vibrations occur at frequencies lower than those of A_{1g}^2 and E_g^2 . The latter modes, where the outer Bi/In and Se^1 atoms move in opposite phase, are mainly affected by the forces between Bi/In and Se^1 atoms. In E_g^1 and A_{1g}^1 modes, the outer Bi/In– Se^1 pairs move in phase. Thus, the Bi/In– Se^2 bonding forces are primarily involved in these vibrations. The observed Raman optical phonons peaks were identified as A_{1g}^1 ($\sim 78\text{ cm}^{-1}$), E_g^2 ($\sim 130\text{ cm}^{-1}$) and A_{1g}^2 ($\sim 170\text{ cm}^{-1}$) similar to the previously reported ones [45–50]. Each of the E_g and A_{1g} modes are 2-fold degenerate. In these phonon modes, the atoms vibrate in-plane and out-of-plane respectively [47].

4. Conclusion

In this work, nominal bulk $\text{In}_x\text{Bi}_{40-x}\text{Se}_{60}$ ($1.6 \leq x \leq 13.2$) materials are successfully prepared and characterized. The physical

parameters namely the coordination number Z, the number of constraints N_s , the compactness δ and the parameter R are evaluated from the stoichiometry and density measurements. These parameters are found to be well-correlated with topological and chemical ordered network models. The XRD data reveal presence of the rhombohedral phase of $(\text{Bi}, \text{In})_2\text{Se}_3$ and complete absence of other phases. The XRD and Raman spectroscopy analyses suggest existence of two basic structural units, $\text{Bi}(\text{In})\text{Se}_3$ pyramids with threefold coordinated Bi (In) atom at the apex. This study illustrates the utility of Raman spectroscopy to investigate how the compositional variations due to In-doping affect the lattice vibrations and the electron phonon interactions in the layered Bi_2Se_3 samples.

Acknowledgements

S. A. Saleh express appreciation for the financial support to this work from the Deanship of Scientific Research, Najran University, Najran, Saudi Arabia, in the form of research project (Project no. 9/10).

References

- [1] B. Pejova, I. Grozdanov, Thin Solid Films 408 (2002) 6–10.
- [2] D.B. Hyun, J.S. Hwang, T.S. Oh, J.D. Shim, N.V. Kolomoets, J. Phys. Chem. Solids 59 (1998) 1039.
- [3] C.B. Bates, L. England, Appl. Phys. Lett. 14 (1996) 390.
- [4] R.N. Bhattacharya, P. Pramanik, J. Electrochem. Soc. 129 (1982) 332.
- [5] S.A. Ahmed, E.M.M. Ibrahim, S.A. Saleh, Appl. Phys. A 85 (2006) 177–184.
- [6] M.A. Abdel-Rahim, M.M. Hafiz, A.M. Shamekh, Physica B 369 (2005) 143–154.
- [7] V.D. Das, P.J. Lakshmi, Phys. Rev. B37 (1988) 720.
- [8] S. Mahadevan, A. Giridhar, A.K. Singh, J. Non-Cryst. Solids 88 (1986) 11.
- [9] N. Afify, M.A. Abdel-Rahim, A.S. Abd-El-Halim, M.M. Hafiz, J. Non-Cryst. Solids 128 (1991) 269.
- [10] S.A. Saleh, Mater. Sci. Appl. 2 (2011) 950.
- [11] (a) J.C. Phillips, J. Non-Cryst. Solids 34 (1979) 153;
(b) J.C. Phillips, J. Non-Cryst. Solids 43 (1981) 37.
- [12] P. Tronc, M. Benoussan, A. Brenac, C. Sébennet, Phys. Rev. B 8 (1973) 5947.
- [13] G. Lucovsky, F.L. Galeener, R.C. Keezer, R.H. Geils, H.A. Six, Phys. Rev. B 10 (1974) 5134.
- [14] J. Bicerano, S.R. Ovshinsky, J. Non-Cryst. Solids 74 (1985) 75.
- [15] S. Sen, E.L. Gjersing, B.G. Aitken, J. Non-Cryst. Solids 356 (2010) 2083–2088.
- [16] http://www.knovel.com/web/portal/periodic_table
- [17] V. Pamukchieva, E. Savova, Thin Solid Films 347 (1999) 226.
- [18] M. Fadel, Vacuum 48 (1997) 73.
- [19] J. Bicerano, S.R. Ovshinsky, Chemical bonding and the nature of glass structure, in: V.H. Smith Jr., H.F. Schaefer, K.D. Morokuma (Eds.), Applied Quantum Chemistry, Reidel Publishing Company, Holland, 1986.
- [20] Ambika, P.B. Barman, J. Ovonic Res. 3 (2007) 21.
- [21] <http://www.periodni.com/en/index.html>
- [22] A. Dahshan, K.A. Aly, Philos. Mag. 88 (2007) 361.
- [23] G. Saffarini, Physica B 253 (1998) 52–55.
- [24] V. Pamukchieva, A. Szekeres, K. Todorova, M. Fabian, E. Svab, Zs Revay, L. Szentmiklosi, J. Non-Cryst. Solids 355 (2009) 2485–2490.
- [25] N. Yamaguchi, Philos. Mag. 51 (1985) 651.
- [26] E.A. Davis, H. Wright, N.J. Doran, C.M.M. Nex, J. Non-Cryst. Solids 32 (1979) 257.
- [27] H.K. Rockstadt, Bull. Am. Phys. Soc. 16 (1971) 304.
- [28] A.M. Farid, S.S. Fouad, A.H. Ammar, J. Mater. Sci. Mater. Elect. 16 (2005) 97.
- [29] A. El-Korashy, A. Bakry, M.A. Abdel-Rahim, M. Abd El-Sattar, Physica B 365 (2005) 55.
- [30] S. Mahadevan, A. Giridhar, A.K. Singh, J. Non-Cryst. Solids 103 (1988) 179.
- [31] J.C. Phillips, M.F. Thorpe, Solid State Commun. 53 (1985) 699.
- [32] Z.A. Ali, G.H. Adel, A.S. Abd-rbo, Chalcogenide Lett. 6 (2009) 125.
- [33] S. Augustine, S. Ampili, J.K. Kang, E. Mathai, Mater. Res. Bull. 40 (2005) 1314.
- [34] R.D. Shannon, C.T. Prewitt, Acta Crystallogr. B25 (1969) 925.
- [35] S.A. Saleh, Physica C 444 (2006) 40.
- [36] M.M. Ibrahim, E.M.M. Ibrahim, S.A. Saleh, A.M. Abdel Hakeem, Alloys Comp. J. 429 (2007) 19–24.
- [37] J. Dheepa, R. Sathyamoorthy, S. Velumani, A. Subbarayan, K. Natarajan, P.J. Sebastian, Sol. Energy Mater. Sol. Cells 81 (2004) 305–312.
- [38] S. Subramanian, D.P. Padiyan, Mater. Chem. Phys. 107 (2008) 392–398.
- [39] F. Gu, S.F. Wang, M.K. Lu, G.J. Zhou, D. Xu, D.R. Yuan, J. Phys. Chem. B 108 (2004) 8119–8123.
- [40] V. Biju, N. Sugathan, V. Vrinda, S.I. Salini, J. Mater. Sci. 43 (2008) 1175–1179.
- [41] C. Karunakaran, S.S. Raadha, P. Gomathisankar, J. Alloys Compd. 549 (2013) 269–275.
- [42] L. Pauling, The Nature of the Chemical Bond, Cornell University Press, Ithaca, NY, 1960.
- [43] E. Mytilineou, B.S. Chao, D. Papadimitriou, J. Non-Cryst. Sol. 195 (1996) 279–285.

- [44] S.A. Saleh, A. Al-Hajry, H.M. Ali, *Phys. Scr.* 84 (2011) 015604.
- [45] D. Teweldebrhan, V. Goyal, M. Rahman, A.A. Balandin, *Appl. Phys. Lett.* 96 (2010) 053107.
- [46] W. Richter, H. Kohler, C.R. Becker, *Phys. Status Sol. B* 84 (1977) 619.
- [47] A. Soni, Z. Yanyuan, Y. Ligen, M.K.K. Aik, M.S. Dresselhaus, Q. Xiong, *Nano Lett.* 12 (2012) 1203–1209.
- [48] K.M.F. Shahil, M.Z. Hossain, D. Teweldebrhan, A.A. Balandin, *Appl. Phys. Lett.* 96 (2010) 153103.
- [49] V. Russo, A. Bailini, M. Zamboni, M. Passoni, C. Conti, C.S. Casari, A. Li Bassi, C.E. Bottani, *J. Raman Spectrosc.* 39 (2008) 205.
- [50] E. Kh Shokr, E.M.M. Ibrahim, A.M. Abdel Hakeem, A.M. Adam, *J. Exp. Theor. Phys.* 116 (2013) 166–172.